Effectiveness of Resilience Index in Assessing Power System Performance

Hasna Satya Dini and Jasrul Jamani Jamian

Abstract The prediction of disaster increment in the upcoming year requires a proper strategy to prevent a widespread impact in electrical network. Quantitative, risk-based metrics are essential for capturing a power system condition during the planning, operating, and recovering stages of a disaster. Several studies have been conducted to develop strategy in quantifying resilience condition in electrical network. Yet, none of those indices nor method has been widely approved as a worldwide standard. Thus, this paper attempts to evaluate several resilience metrics, namely RICD, *Ri*, *Rt*, and *R*time, during a disaster in four different scenarios. The goal of this analysis was to seek the most appropriate index which will be able to capture the whole parameter of electrical system resilience. Typhoon Vicente is used as sample disaster on IEEE 6 bus power system which overlaid on South China area. The simulation shows that the resilience indices that are tested show significant different values for all resilience indices in each scenario. RICD and *R*time have a strong influence from the comparison of typhoon duration and total repair time, while the amount of loss load has a stronger influence on *Ri* and *Rt*. Thus, a new index that is able to capture both phenomenon is needed to capture the full picture of power system during disaster.

Keywords Resilience · Index · Disaster · RICD · Transmission

H. S. Dini (✉) · J. J. Jamian
Universiti Teknologi Malaysia, Skudai, Malaysia
e-mail: hasna@graduate.utm.my

J. J. Jamian
e-mail: jasrul@utm.my

H. Malik et al. (eds.), *Renewable Power for Sustainable Growth*,
Lecture Notes in Electrical Engineering 1086,
https://doi.org/10.1007/978-981-99-6749-0_68

1 Introduction

Greenhouse gases emission causes an increase in air and water temperatures worldwide. Based on research, it is predicted that there will be an increase in the quantity and capacity of hurricanes, winter storms, heat waves, floods, and other disasters which are posing a threat to the global sustainability of environmental, infrastructure, and even economic system [1, 2]. For example, Hurricane Sandy caused the loss of access to electricity for 7 million people in 2012. This disaster destroyed over 100,000 main power lines. Several transformers at substations exploded and flooded substations. During 2010–2011, Queensland, Australia, experienced flooding, which affected six transformer substations. The disaster is estimated to have caused more than 150,000 customers to lose access to electricity. In 2008, China experienced an ice storm disaster that caused damage to 2000 substations and destroyed 8500 poles which caused a loss of access to electricity in 13 provinces and 170 cities [3].

The strong impact of natural disasters on access to electricity causes the need for a proper strategy to prevent the widespread of its impact. Conventional reliability calculations become irrelevant because they are based on the $N-1$, $N-2$, or $N-n$ contingency. Meanwhile, as mentioned in the paragraph above, natural disasters with a low probability and high impact can cause loss of components up to N-40. An index that can accommodate system readiness prior to these events is important so that prevention and mitigation can be carried out effectively by knowing the system's condition. In this case, resilience is offered as an index to quantify system readiness to face high-impact low-probability disasters.

Resilience in electricity is defined as the capability of a power system to plan to absorb, recover, and successfully adapting to adverse event [4]. Resilience in power system can be evaluated at infrastructure or electrical system level to develop methodologies which provide information to electrical operator and owner [5]. Quantitative, risk-based metrics are essential for measuring a system during the planning, operating, and recovering stages of a disaster. The results of this calculation will be the basis for determining policies, planning, operations, and investment in electric power systems [6]. Several studies have attempted to develop a metric for calculating resilience [7]. However, the metrics for calculating resilience in electric power systems have yet to agree on a standard.

Several resilience proposed indices were presented in [4] including resilience function which evaluate the system using trapezoidal performance or triangle performance. The paper gave a brief explanation about each of the index yet, and it did not simulate the disaster event to review the difference between those indices accurately. In [6], resilience indices which evaluate different aspect of resilience were assessed. It presented capacity resilience indices, speed recovery resilience indices, grid recovery resilience indices, and grid improvement parameter under Typhoon Boyalen and Typhoon Saba. The grid functionality difference between two events is used to observe system's improvement. These indices were meant to give a complete explanation of system resilience.

The development of some proposed resilience indices made it necessary to compare the effectiveness of them. Without this analysis, the reader will not be able to determine the difference between each indices and pick the proper index which properly captures the system's resilience condition. Thus, this paper attempts to evaluate several resilience metrics during a disaster in four different scenarios. The disaster is simulated in the electrical system, and the system response will be evaluated. The value of each metric will be compared to see the effectiveness in a different disaster scenario.

The structure of this paper is as follows: Sect. 2 describes the concept of resilience in general, and Sect. 3 contains the steps taken in the simulation and scenario variations. Section 4 contains the procedures for modeling the components and sampled disasters. Section 5 displays the simulation data, and Sect. 6 contains an analysis of the simulation results. Section 7 contains a discussion of the result, and Sect. 8 is the conclusion and next steps to be taken.

2 Concept of Resilience

2.1 Definition of Resilience

A multi-phase resilience trapezoid curve can describe the impact of disturbances on the power system [8]. The trapezoidal curve in Fig. 1 depicts each phase of the disaster as follows:

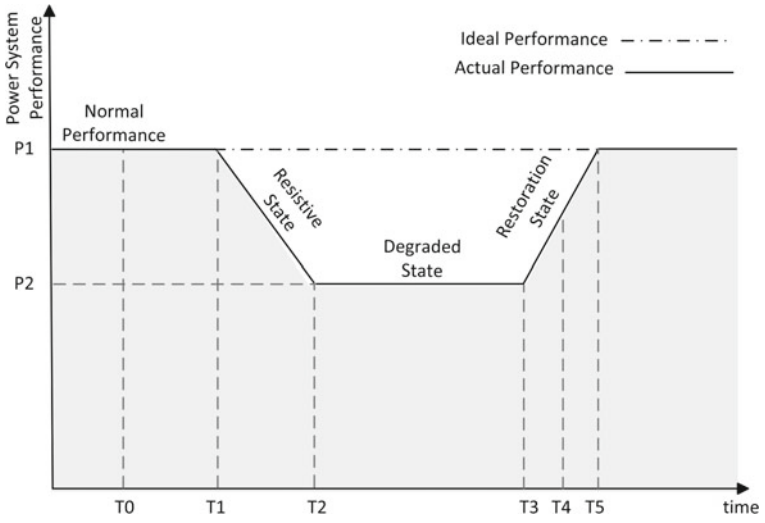

Fig. 1 Trapezoidal resilience curve

- Phase 1 is the initial phase of disturbance (T0), where the system can still maintain its performance as normal. Phase 1 ends when deterioration in system performance (T1) begins. In this phase, the system's strength is tested when a disturbance occurs. In a good system, phase 1 will last a long time; meanwhile, in a poor system, this phase occurs shortly since the component will instantly damage during the early phase of disturbance.
- Phase 2 is a resistive state which starts when a decrease in system performance occurs (T1) until the system reaches its minimum performance (T2). During this phase, the damage of the disturbance reaches the maximum point.
- Phase 3 is a degraded state. In this phase, the system waits for the repair team to make improvements (T3). The faster the repair team responds, the narrower this phase will be.
- Phase 4 is a restoration state, starting from T3 and ending when system performance returns to its normal state at T5. The restorative steps include infrastructure repairs and system reconfiguration (network maneuvers, generator re-dispatch, and micro-gird formation). T4 is when the disturbance is over, which may occur before or after T5. In this phase, system flexibility and speed of restoration will be seen.

2.2 Resilience Metrics

Based on the four phases mentioned, a resilience matrix needs to describe the conditions of each phase. The resilience calculation that has been developed attempts to describe the overall system resilience in a complete picture. In [8, 9], the traditional reliability index is used to represent system resilience, such as loss of load probability (LOLP), expected demand not served (EDNS), and expected energy not served (EENS). The calculation process employs the Monte Carlo method to produce those indices. While new indices were introduced in [10], the system's resilience performance was evaluated using (1).

$$R = E\left[\frac{\sum_{n=1}^{N} T_u}{\sum_{n=1}^{N} T_u + T_D}\right] \tag{1}$$

Load outage duration is represented as T_D, while T_u stands for the load period during up-time, and the symbol N stands for the number of loads connected to the system. A different quantification approach was introduced in [11], and that resilience is the ratio of the area under the actual performance curve to the area under ideal performance, as shown in **Error! Reference source not found.**:

$$R_t = E\left[\frac{\int_{T_1}^{T_5} \mathrm{AP}(t)\mathrm{d}t}{\int_{T_1}^{T_5} \mathrm{IP}(t)\mathrm{d}t}\right] \tag{2}$$

Equation (2) misses to capture the system resistance [12]. A part of the system resistance is tested between $[T_0, T_1]$. The disaster has already occurred in this period, but the system can sustain its previous performance. Reference [13] has a quite similar approach to (2), yet it is able to consider the system resistance using the equation below:

$$R_i = E\left[\frac{\int_{T_0}^{T_5} \mathrm{AP}(t)\mathrm{d}t}{\int_{T_0}^{T_5} \mathrm{IP}(t)\mathrm{d}t}\right] \tag{3}$$

AP in (3) represents the system's actual performance, and the performance may be represented using the supplied load. The actual and ideal performance (IP) is integrated from the beginning of the disturbance (T_0) to the time during the system reaches its previous performance (T_5). The resilience index presented in [12] (RICD) of a transmission network adds an essential part from (3) as follows:

$$R_{\mathrm{icd}} = E\left[\frac{\int_{T_0}^{T_5} \mathrm{AP}(t)\mathrm{d}t}{\int_{T_0}^{T_5} \mathrm{IP}(t)\mathrm{d}t}\,\frac{T_4 - T_0}{T_5 - T_0}\right] \tag{4}$$

Another approach is also introduced in evaluating system resilience to determine the impact of improvement. In [14], to measure system resilience during penetration of distributed generation using renewable energy sources, the system resilience is quantified using a fraction of the load buses whose voltage deviation is beyond ± 5% of its nominal voltage to all load buses.

3 Design of Methodology

Initial steps started with modeling the electric power system components, both on the structural and electrical sides. Infrastructure model of transmission line strength was employing normal logarithmic equation, while electrical network is using [15] model to simulate power flow analysis. The disturbances, in this case typhoon storms, are also modeled in spatial and temporal using a modified Rankine Vortex. The strength of the components is compared with the wind speed experienced per unit of time. The system's performance will be evaluated when a component cannot survive.

The resilience value was calculated using the Monte Carlo method, where the simulation was carried out 1000 times to ensure convergent results. The simulation steps can be seen in Fig. 2.

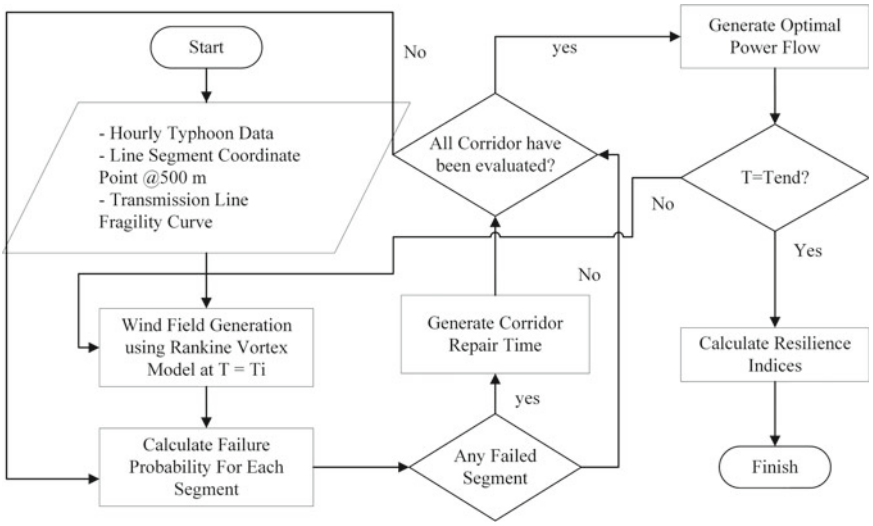

Fig. 2 Design of methodology

In this simulation, four scenarios will be used:

1. Scenario 1 (normal condition)

Under normal conditions, the number of teams is assumed to be only 1. If multiple outages occur, the next component shall wait until the repair team is available. The repair speed is 1 h per 500 m transmission line segment, and the speed of the repair team to arrive at the point of damage is 60 m/s.

2. Scenario 2 (component robustness variation)

In scenario 2, the strength variation of the transmission line is carried out where the strength is varied for normal (37 m/s), low (32 m/s), and strong (42 m/s) values. The four methods are calculated for each strength.

3. Scenario 3 (repair team variation)

The simulation is conducted for different numbers of repair teams. In normal conditions, only 1 team is available. For another case, we increase the number of the team into 2 teams, 4 teams, and in extreme conditions, 100 teams are employed.

4. Scenario 4 (repair speed variation)

In the last scenario, the repair speed is varied. For normal conditions, the repair speed is 1 h per transmission line segment (500 m). In other cases, the repair speed is simulated for 2 h per segment, 4 h per segment, and half an hour per segment.

The result of resilience indices between all four scenarios was then compared to see their effectiveness.

4 Evaluation of Typhoon Impact to Power System

4.1 Typhoon Modeling

Typhoon is a natural phenomenon that is difficult to be completely described. Even though wind measurements can be obtained from satellites or aircraft, it has yet to be possible to describe the three-dimensional model of the cyclone. Thus, a two-dimensional parametric model is often used to facilitate analysis in typhoon modeling. In [16], a parametric wind modeling method was compared: Rankine Vortex, Slosh, and Holland, where it was found that Rankine Vortex provided the best model when compared to the other two models.

Wind speed will be zero at the storm's center and increase as it gets closer to the maximum speed point, then decrease as the position is further away from the maximum point. The modified Rankine Vortex describes the wind speed distribution using Eq. (5).

$$\begin{aligned} V &= V_{\max}\left(\frac{r}{R_{\mathrm{mw}}}\right)^{X} \quad \text{for } r < R_{\mathrm{mw}} \\ V &= V_{\max}\left(\frac{R_{\mathrm{mw}}}{r}\right)^{X} \quad \text{for } r \geq R_{\mathrm{mw}} \end{aligned} \tag{5}$$

The variable $V_{\max}$ indicates the maximum speed of the typhoon in the specified time. While R_{mw} is the distance from the typhoon's center to its maximum velocity point, r is the distance from the typhoon's center to the observed point. Parameter X adjusts the wind speed distribution and has a value range of $0.4 < X < 0.6$. In this case, the average value is 0.5.

The calculated wind speed needs to be adjusted at a standard 10-m height using Eq. (6), with K_m being a correction factor of 0.8 in the modified Rankine Vortex modeling.

$$V_{10} = K_m V \tag{6}$$

The wind speed is assumed to have a circular wind flow, which is insufficient to depict the actual wind direction. The correction of wind direction shall be made using Eq. (7).

$$\begin{aligned} \beta &= 10^{\circ}\left(1 + \frac{r}{R_{\mathrm{mw}}}\right) \quad \text{for } 0 \leq r \leq R_{\mathrm{mw}} \\ \beta &= 20^{\circ} + 25^{\circ}\left(\frac{r}{R_{\mathrm{mw}}} - 1\right) \quad \text{for } R_{\mathrm{mw}} \leq r \leq R_{\mathrm{mw}} \\ \beta &= 10^{\circ}\left(1 + \frac{r}{R_{\mathrm{mw}}}\right) \quad \text{for } 0 \leq r \leq R_{\mathrm{mw}} \end{aligned} \tag{7}$$

The cyclone's forward motion shall be accounted for using Eq. (8). V_f is the forward velocity of typhoon movement, and U is the correction term.

$$U = \frac{R_{\text{mw}} r}{R_{\text{mw}}^2 + r^2} V_f \tag{8}$$

Thus, the total wind speed that affected the transmission line will be obtained in Eq. (9).

$$V_r = V_{10} + U \tag{9}$$

4.2 Component Modeling

The fragility curve will represent the strength of the transmission line when there is a typhoon. In [17], a logarithmic trend exists between wind speed and the probability of component failure. Thus, the failure probability of the transmission line can be represented by the normal logarithmic Eq. (10).

$$P_{1i} = \Phi(v) \tag{10}$$

With an average value of 37 and a standard deviation of 5 [12], this fragility curve represents the strength of the transmission line segments with a length of 500 m per segment.

4.3 Repair Process

The repair process of the components considers wind speed impact. A longer repair time (TTR) is needed at higher speed values. The total time to repair will include component repair time, waiting time, and time the repair team needs to reach the damaged area [12].

1. The wind speed impact is considered in the time to repair (TTR) using the
2. The TTR of the component will depend on the wind speed represented in the coefficient (k) as stated in Eq. (11).

$$\text{ttr}_m = \text{ttr}_{\text{norm}} \times k \tag{11}$$

3. The repair team's required time to reach the repair area is added to the total repair time, where the length of travel time will depend on the distance of the repair team from the disturbance point (d) and the speed of the repair team to

the disturbance point v_r as in Eq. (12).

$$t_r = \frac{d}{v_r} \tag{12}$$

4. Component repairs will be carried out alternately, with which the first failure will be served first so that the t_{wait} will be added to the total repair time as in Eq. (13).

$$\text{ttr}_{\text{total}} = (\text{ttr} + t_r) \times k + t_{\text{wait}} \tag{13}$$

5 Simulation Data

The synthetic data is acquired using open-source data that is available online.

5.1 Typhoon Data

The simulated typhoon data is Vicente Typhoon that occurred from 21 June 2012 to 25 June 2012, taken from [18] and given in Table 1. Since forward motion data to solve (8) is not provided, it is estimated using the distance from the typhoon center between two consecutive data points divided by 6 h (time interval between two data points).

5.2 Electrical System Data

The tested system data is the reliability test system, IEEE 6 bus [19], which overlaid on the typhoon-impacted area. Figure 3 illustrates the IEEE 6 buses overlaid in the South China area, and Table 2 shows coordinate points of each bus.

5.3 Restoration Procedure

The system repair procedure is carried out based on sub-chapter IV-3, where the repair team is assumed to be on Substation 5 (113.06°E, 22.61°N). The value of the multiplier coefficient will depend on the wind speed by following the normal distribution in Eq. (14).

Table 1 Simulated typhoon data

Time	Lat (deg.)	Long (deg.)	V_{max} (knot)	Rc (km)	R_{max} (km)
2012-7-20 06:00	18	123	20	0	0
2012-7-20 12:00	19	122	20	0	0
2012-7-20 18:00	20	122	20	0	0
2012-7-21 00:00	20	120	25	315	83
2012-7-21 06:00	20	118	20	333	83
2012-7-21 12:00	19	117	30	333	83
2012-7-21 18:00	19	116	40	315	83
2012-7-22 00:00	19	116	45	333	65
2012-7-22 06:00	19	115	45	333	65
2012-7-22 12:00	19	115	45	333	56
2012-7-22 18:00	19	115	50	315	56
2012-7-23 00:00	20	115	50	333	37
2012-7-23 06:00	21	115	65	333	46
2012-7-23 12:00	21.10	114.20	80	291	28
2012-7-23 18:00	21.70	113.30	115	296	28
2012-7-24 00:00	22.30	112.30	85	296	28
2012-7-24 06:00	23	111	60	296	28
2012-7-24 12:00	23	109	45	0	0
2012-7-24 18:00	24	107	45	0	0
2012-7-25 00:00	24	105	20	0	0

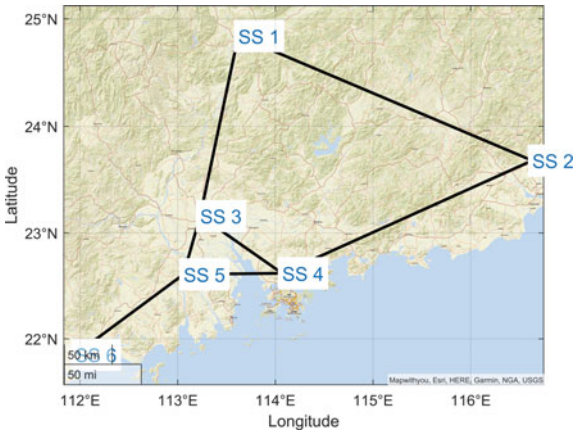

Fig. 3 IEEE 6 bus test system overlaid on South China

Table 2 IEEE 6 bus substation coordinate

SS	1	2	3	4	5	6
Long	113.62°	116.63°	113.23°	114.07°	113.06°	111.95°
Lat.	24.84°	23.68°	23.16°	22.62°	22.61°	21.85°

$$k_w = \begin{cases} 1 & 0 \le v \le 10 \text{ m/s} \\ U(1,2) & 10 \text{ m/s} < v \le 20 \text{ m/s} \\ U(2,3) & 20 \text{ m/s} < v \le 40 \text{ m/s} \\ U(3,4) & 40 \text{ m/s} < v \le 60 \text{ m/s} \\ U(4,5) & 60 \text{ m/s} < v \end{cases} \tag{14}$$

6 Analysis of Typhoon Impact

6.1 Scenario 1

Under normal circumstances, the resilience index is obtained using 1000 simulations to achieve convergence of values as shown in **Error! Reference source not found.** using Eqs. (2), (3), and (4) and the elements of Eq. (4) as shown in Eq. (15).

$$R_{\text{time}} = E\left[\frac{T_4 - T_0}{T_5 - T_0}\right] \tag{15}$$

The typhoon is impacting the transmission line between Substations 5 and 6 (lines 5–6). During first simulation, 60 segments were failed and need immediate repair action, while other transmission line did not experience any failure in the segment. The failure in lines 5–6 causes system to loss load in Substation 6 (20 MW) due to unavailability of power generation back up in that substation. The system able to restore to its previous performance in hour 154 after disturbance in the first simulation is depicted in Fig. 4.

The simulation result is shown in Fig. 5, showing a similar value between *R*icd (4)–*R*time and *Ri* (3)–*Rt* (2). The *R*icd and *R*time show a relatively low resilience index since restoration time is much longer than the typhoon duration. *Ri* and *Rt* have higher value because the system can sustain most of its load, and the restoration time does not significantly impact it.

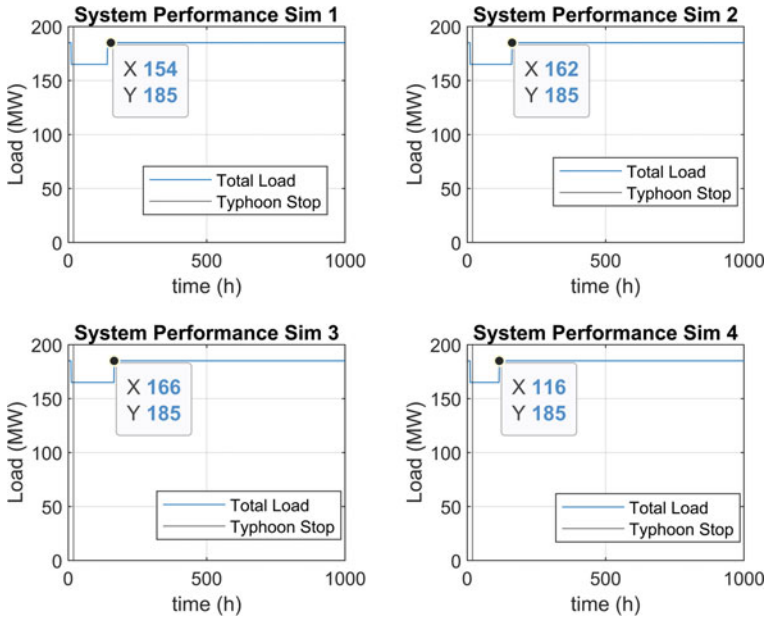

Fig. 4 Snapshot of system performance in normal condition for the first four iterations

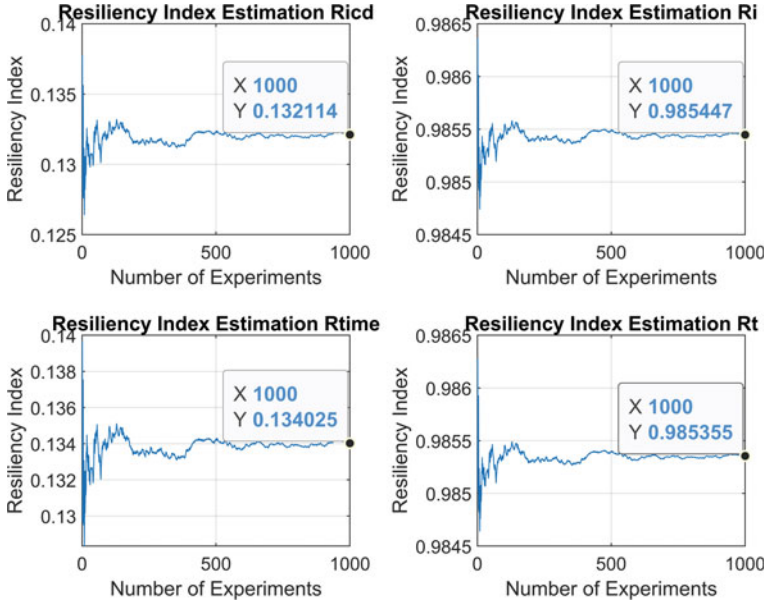

Fig. 5 Resilience index estimation *R*icd, *Ri*, *R*time, and *Rt*

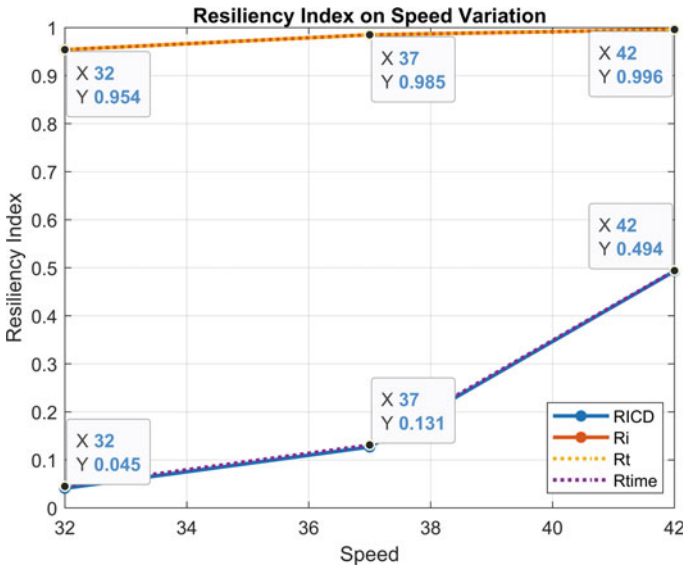

Fig. 6 Resilience index graph scenario 1

6.2 Scenario 2

In scenario 2, variations were made on the robustness of the transmission line. The scenario is done by changing the wind speed to 32 and 42 m/s so that the results are shown in Fig. 6. There is an increase in the value of the resilience indices in the four calculation methods when the strength of the transmission line increases. The significant difference to normal condition occurs in the *R*ICD and *R*time values, which are 0.131–0.494, whereas in the *Ri* and *Rt* conditions, the value is not substantially different from 0.985 to 0.996. The insignificance occurs due to the loss of load in scenario 2, and normal scenario is similar, and the faulty segment only occurs in line 9 resulting unsupplied load in bus 6.

Meanwhile, when the transmission line strength drops by 5 m/s, the resilience values on *Ri* and *Rt* drop significantly to 0.045. The value is declining because the number of broken transmission line segment in the first simulation is 140 segments which result system able to restore its supplied load in hour 456.

6.3 Scenario 3

In scenario 3, variations are made on the number of repair teams using 2 teams, 10 teams, and an extreme case of 100 teams. In case of using 2 repair teams, it was seen that the repair was completed at 185 h, and the typhoon stopped at 20 h.

Meanwhile, an interesting thing occurred when 100 teams worked together to repair the faulty components. In Fig. 7, the repair finished in 15 h which preceded the typhoon duration. This phenomenon causes the resilience value on the *R*ICD and *R*time methods to exceed the expected maximum value (1) to 1.343 as depicted in Fig. 8.

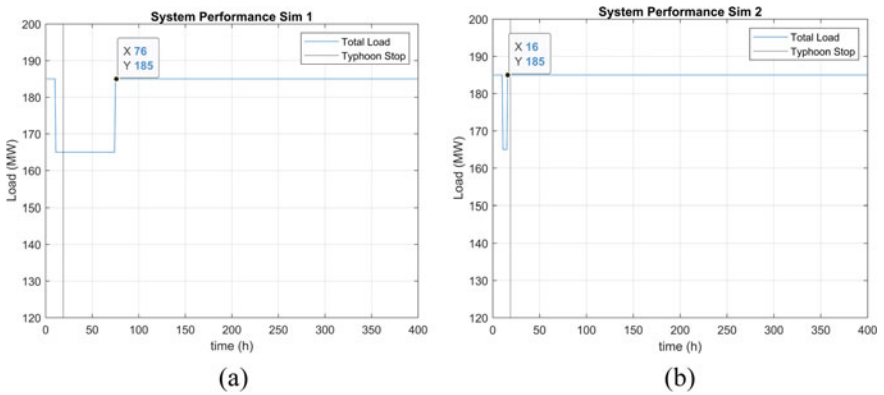

Fig. 7 Snapshot of single simulation **a** 2 repair teams **b** 100 repair teams

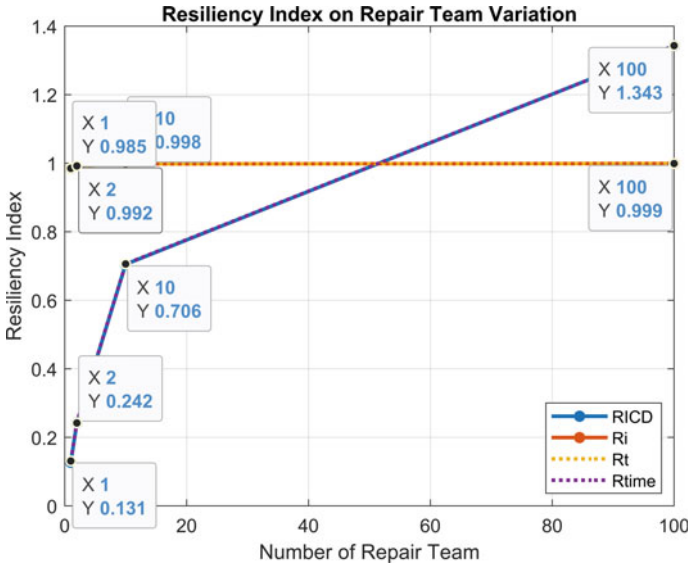

Fig. 8 Resilience index graph scenario 2

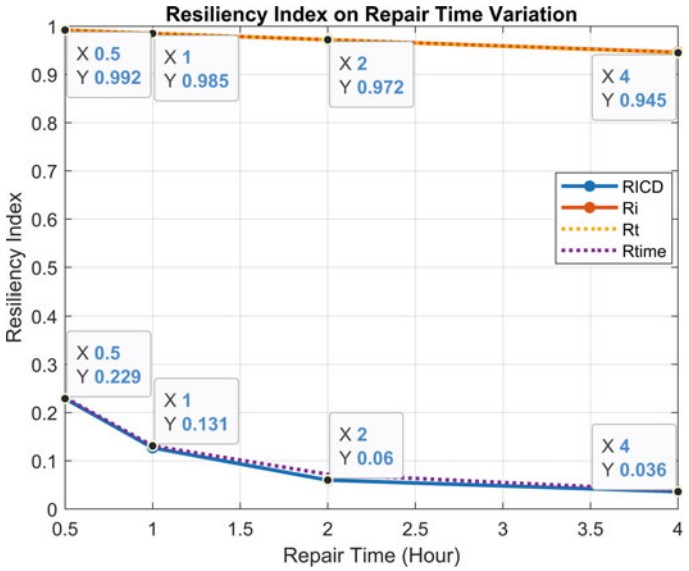

Fig. 9 Resilience index graph scenario 3

6.4 Scenario 4

In scenario 4, variations in repair time that are carried out with repair time per 500 m transmission line segment are 0.5, 2, and 4 h. The longer the repair time, the lesser resilience indices on the four methods. *R*icd and *Ri* experienced a significant decrease of about 50% in value when the repair duration was 2 times longer than normal conditions. Meanwhile, the decline was insignificant for *Ri* and *Rt*, from 0.985 to 0.972 and 0.945 as shown in Fig. 9, respectively. When the repair time was accelerated to 0.5 h, the resilience increased significantly in *R*icd and *R*time to 0.229 and 0.231 from the previous 0.127 and 0.131.

7 Discussion

Based on simulations in all scenarios, a very significant difference exists between *R*icd–*R*time and *Ri*–*Rt*. The value of *R*icd and *Rt* is greatly influenced by the comparison between the time of the typhoon duration and the total repair time $\frac{T_{\text{dur}}}{T_5 - T_0}$. *Ri* and *Rt* are more affected by the load lost during the disturbance. Even though the repair time is longer, the decrease in the value of resilience is not significant because the proportion of lost load is small compared to the load that survived when the disturbance occurred. However, the *R*icd and *Rt* calculations show overly time-sensitive results. The resilience value is significantly low even though the load loss proportion is only 11% to the entire load.

8 Conclusion and Future Work

In this paper, we have tested the effectiveness of four methods of calculating efficiency using the Monte Carlo method. The simulation was conducted by simulating Typhoon Vicente on the overlaid IEEE 6 bus network in the South China area. In the four methods tested, *R*ICD–*R*time and *Rt*–*Ri* have similarities. *R*icd and *R*time are highly sensitive to the comparison of the typhoon duration to the total repair duration. Thus, even if the loss load is small, the resilience index value will be small if the repair time is much longer than the typhoon duration (loss of only 11% load but resilience could be < 0.01). However, for *Rt* and *Ri*, the resilience values do not sufficiently reflect the repair time differences. These two indices highly influenced y amount of loss load; as long as the loss load is similar, the resilience indices will not have a significant difference.

Based on this simulation, it is necessary to have a resilience index that can fully describe the system's strength and the length of time for repairs proportionally. Thus, for future work, the author will do research to compose a resilience index that is able to capture both phenomena.

References

1. President EOOT (2013) Economic benefits of increasing electric grid resilience to weather outages, T.W. House, Washington
2. Shammin MR, Haque AKE, Faisal IM (2022) A framework for climate resilient community-based adaptation. Climate change and community resilience. Springer, Singapore, pp 11–30
3. Panteli M, Mancarella P (2015) The grid: stronger, bigger, smarter? In: IEEE power and energy magazine. IEEE, pp 58–66
4. Izadi M et al (2020) A critical reveiew on definitions, indices, and uncertainity charaterization in resiliency-oriented operation of power system. Int Trans Electr Energy Syst 30(1):1–28
5. Alam MM, Eren Tokgoz B, Hwang S (2019) Framework for measuring the resilience of utility poles of an electric power distribution network. Int J Disast Risk Sci 15:270–281
6. Jufri FH, Widiputra V, Jung J (2019) State-of-the-art review on power grid resilience to extreme weather events: definitions, framework, quantitative assessment methodologies, and enhancement strategies. Appl Energy 239:1049–1065
7. Mathaios Panteli PM (2015) Influence of extreme weather and climate change on the resilience of power systems: impacts and possible mitigation strategies. Electr Power Syst Res 127:259–270
8. Panteli M et al (2017) Metrics and quantification of operational and infrastructure resilience in power systems. IEEE Trans Power Syst 32(6):4732–4742
9. Younesi A et al (2020) A quantitative resilience measure framework for power systems against wide-area extreme events. IEEE Syst J 16(1):915–922
10. Kwasinksi A (2016) Quantitative model and metrics of electrical grids' resilience evaluated at a power distribution level. Energies 9(2):93
11. Ouyang M, Min X (2012) A three-stage resilience analysis framework for urban infrastructure systems. Struct Saf 36–37(2):23–32
12. Yang Y et al (2018) Quantitative resilience assessment for power transmission systems under typhoon weather. IEEE Access 6:40747–40756

13. Mousavizadeh S, Mahmoud-Reza S, Mohammad-Hossein A (2017) A linear two-stage method for resiliency analysis in distribution systems considering renwable energy and demand response resource. Appl Energy 211:443–460
14. Scala A, Mureddu M, Chessa A, Caldarelli G, Damiano A (2013) Distributed generation and resilience in power grids. In: Hämmerli BM, Kalstad Svendsen N, Lopez J (eds) Critical Information Infrastructures Security. Springer, New York, pp 71–79
15. Saadat H (1999) Power system analysis. The McGraw-Hill Companies, New York
16. Phadke AC et al (2003) Modeling of tropical cyclone winds and waves for emergency management. Ocean Eng 30:553–578
17. Krisy Murray KRWB (2014) Wind related faults on the GB transmission network. In: Proceedings of the 2014 international conference on probabilistic methods applied to power systems (PMAPS), pp 1–6
18. Command NMO (2012) Best track western Pacific 12 June 2012. Mississipi
19. Billinton RKS, Chowdhury N, Chu K, Debnath K, Goel L, Khan E, Kos P, Nourbakhsh G, Oteng-Adjei J (1989) A reliability test system for educational purposes-basic data. IEEE Trans Power Syst 4(3):1238–1244